The c_i/b_H moiety in the b_6f complex studied by EPR: A pair of strongly interacting hemes

Frauke Baymann*, Fabrice Giusti†, Daniel Picot†, and Wolfgang Nitschke*‡

*Laboratoire de Bioénergétique et Ingénierie des Protéines, Institut de Biologie Structurale et Microbiologie, Unité Propre de Recherche 9036, Centre National de la Recherche Scientifique, 31 Chemin Joseph-Aiguier, 13402 Marseille Cedex 20, France; and †Institut de Biologie Physico-Chimique, Unité Mixte de Recherche 7099, Centre National de la Recherche Scientifique-Université Paris 7, 13 Rue Pierre et Marie Curie, 75005 Paris, France

Edited by Hartmut Michel, Max Planck Institute for Biophysics, Frankfurt, Germany, and approved November 17, 2006 (received for review July 26, 2006)

X-band EPR features in the region of 90–150 mT have previously been attributed to heme c_i of the b_6 complex [Zhang H, Primak A, Bowman MK, Kramer DM, Cramer WA (2004) *Biochemistry* 43:16329–16336] and interpreted as arising from a high-spin species. However, the complexity of the observed spectrum is rather untypical for high-spin hemes. In this work, we show that addition of the inhibitor 2-*n*-nonyl-4-hydroxyquinoline *N*-oxide largely simplifies heme c_i's EPR properties. The spectrum in the presence of 2-*n*-nonyl-4-hydroxyquinoline *N*-oxide is demonstrated to be caused by a simple $S = 5/2$, rhombic species split by magnetic dipolar interaction ($A_{xx} = 7.5$ mT) with neighboring heme b_H. The large spacing of lines in the uninhibited system, by contrast, cannot be rationalized solely on the basis of magnetic dipolar coupling but is likely to encompass strong contributions from exchange interactions. The role of the H_2O/OH^- molecule bridging heme c_i's Fe atom and heme b_H's propionate side chain in mediating these interactions is discussed.

photosynthesis | electron transfer | quinone reduction | spin–spin interaction

The x-ray structure resolution of the b_6f complexes from the cyanobacterium *Mastigocladus laminosus* (1) and the green alga *Chlamydomonas reinhardtii* (2) revealed the presence of the additional redox cofactor heme c_i in the b_6f complex with respect to its mitochondrial/proteobacterial homologs. Heme c_i is positioned in the Q_i pocket of the enzyme in very close proximity to the n-side heme b_H and is covalently bound to the cytochrome *b* protein by a single thioether linkage to a cysteine residue. No axial ligands are provided by the surrounding protein, and a water molecule or a hydroxide ion is proposed as fifth ligand to heme c_i, based on the crystal structure. Heme c_i's role remains enigmatic at present. Involvements in cyclic electron transfer, redox signaling, state transitions (1, 2), or simply in a variant of Q_i-site turnover have been proposed.

A recent study of isolated cytochrome b_6f complex from *Chlamydomonas* by redox-controlled optical spectroscopy has clarified heme c_i's UV/visible spectral and electrochemical properties (3). The paramagnetic properties of heme c_i, by contrast, are not understood at present. EPR signals in the $g = 6$ region have been interpreted to arise from heme c_i on the basis of their sensitivity to potential exogenous sixth ligands of the putatively 5-coordinated heme (4). The number and field positions of observed lines, however, cannot be rationalized by assuming a single high-spin heme c_i. The unprecedented configuration of the tightly packed pair of redox centers heme c_i/heme b_H, by contrast, may well explain some of c_i's peculiar EPR features.

To progress in our understanding of the paramagnetic properties of this unusual redox center, we have studied the b_6f complex by EPR spectroscopy in the presence and absence of the inhibitor 2-*n*-nonyl-4-hydroxyquinoline *N*-oxide (NQNO) (5) at different redox potentials and in partially ordered samples.

Results

Paramagnetic Species Observed on the Purified b_6f Complex from *Chlamydomonas* and on Spinach Chloroplasts. Fig. 1 shows the EPR spectrum of purified cytochrome b_6f complex from *C. reinhardtii* poised to an ambient redox potential of +200 mV. The spectrum contains contributions from the low-spin hemes *f* and *b* (g_z peaks in the spectral region labeled 2) and from a small fraction of reduced Rieske center (spectral region 3) in addition to several strong lines in the $g = 6$ region (region 1). The positions of the latter signals cover the range of those reported for the *Mastigocladus* enzyme in the untreated state and attributed to heme c_i (4). High-spin hemes typically have superimposed g_x and g_y signals at $g = 6$ (for axial symmetry) or two separate signals around $g = 6$ (in the case of a rhombic center). Substantially more signals are present in this spectral region, and their complex structure as well as the high ($g > 10$) *g* values cannot be explained by a single high-spin heme.

Fig. 2*A* compares EPR spectra of the high-spin spectral region from *Chlamydomonas* membranes, purified b_6f complex from *Chlamydomonas*, and intact spinach chloroplasts and thylakoids. EPR features observed on *Chlamydomonas* membranes and intact spinach chloroplasts cover a narrower field range than those seen in the purified enzyme from *Chlamydomonas* or on thylakoids. In the latter spectra a broad peak at low field values (50–70 mT) can be observed. All samples except the purified enzyme from *Chlamydomonas* give rise to a distinguishable peak at $g = 6.7$, which was also observed in the purified enzyme from spinach and *Mastidogladus* (at $g = 6.6$) (4). The spectra of heme c_i in membranes from *Chlamydomonas* are superimposed by a ramp-shaped signal at $g = 9$, which arises from adventitious iron.

Spectral and Electrochemical Species of Heme c_i in the Presence of NQNO. Fig. 2*B* shows spectacular changes in the spectra induced by the addition of the inhibitor NQNO (5), a semiquinone analogue (6). The numerous resolved and unresolved lines between 40 and at least 155 mT ($g = 13$ to $g = 4$) present in the uninhibited state collapsed to a pair of peaks slightly above $g = 6$ and a derivative shaped line at $g = 5.5$. This action of NQNO corroborates the identification of the low field lines to heme c_i's EPR spectrum, and the similarity of spectra recorded on spinach chloroplast and the purified enzyme from *Chlamydomonas* indicates that the large majority of the high-spin signals in thylakoids seen in Fig. 2*A* are caused by cytochrome b_6f complex.

The simplified spectrum of heme c_i around $g = 6$ in the presence of the inhibitor still shows more lines than expected for a single noninteracting paramagnetic species, which would be a peak and a derivative signal.

Alric *et al.* (3) have recently shown that the Q_i site inhibitor

Author contributions: F.B., D.P., and W.N. designed research; F.B., D.P., and W.N. performed research; F.G. contributed new reagents/analytic tools; F.B. and W.N. analyzed data; and F.B. and W.N. wrote the paper.

The authors declare no conflict of interest.

This article is a PNAS direct submission.

Abbreviations: NQNO, 2-*n*-nonyl-4-hydroxyquinoline *N*-oxide; HP, high-potential; LP, low-potential.

‡To whom correspondence should be addressed. E-mail: nitschke@ibsm.cnrs-mrs.fr.

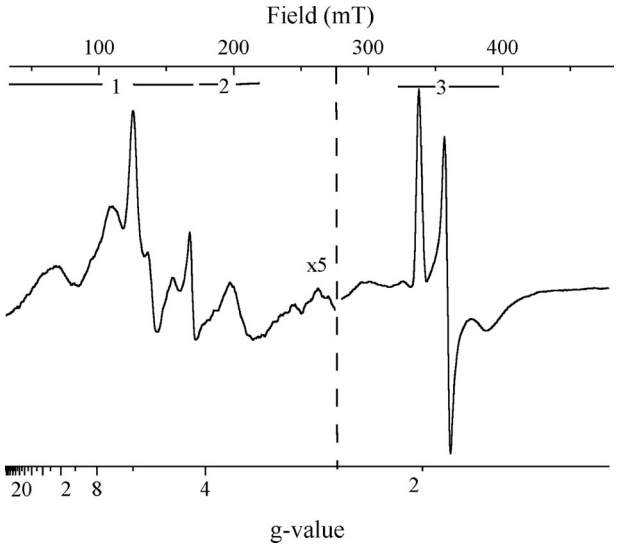

Fig. 1. EPR spectrum of the isolated b_6f complex from *C. reinhardtii* recorded at $E_h = +200$ mV. EPR settings were: temperature, 15 K; microwave power, 2.02 mW; microwave frequency, 9.42 GHz; modulation amplitude, 0.003231 mT; sweep time, 83.89 s. The spectral regions of the $g_{x/y}$ signals of high-spin hemes (1), the g_z signals of cytochromes *b* and *f* (2), and the $g_{z,y,x}$ signals of the Rieske center (3) are indicated. The amplitude in the low-field region has been multiplied by a factor of 5.

NQNO dramatically affects heme c_i's redox properties in optical redox titrations. In the uninhibited enzyme they determined a redox potential of +100 mV at pH 7 and a −60 mV/pH dependence. In the presence of NQNO, two distinct titration waves were observed: The major one titrated at much lower redox potentials ($E_m = -120$ mV), whereas the second one had

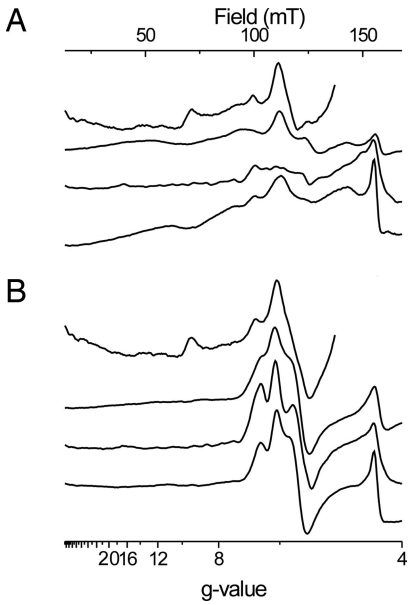

Fig. 2. EPR spectra in the low-field region of (from top to bottom) membranes of *C. reinhardtii*, isolated cytochrome b_6f complex from *C. reinhardtii*, intact chloroplasts, and thylakoids from spinach for an untreated sample (*A*) and in the presence of NQNO (*B*). The amplitude of the signals was normalized to the amplitude of the Rieske spectrum after ascorbate reduction. EPR settings are as for Fig. 1. The amplitude of spectra from *C. reinhardtii* membranes is divided by 2 because they are contaminated by a strong iron signal at $g = 9.35$ and $g = 4.2$.

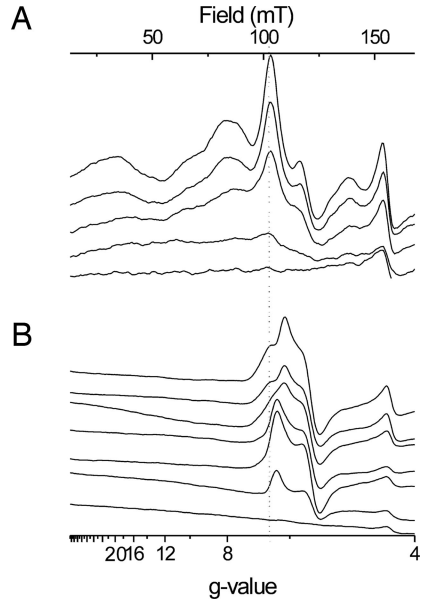

Fig. 3. EPR spectra in the low-field region as recorded during a redox titration of the isolated b_6f complex from *C. reinhardtii* (30 μM). EPR settings are as for Fig. 1. (*A*) Shown are results with no inhibitor; ambient redox potentials from top to bottom are: +362, +198, +18, −104, and −232 mV. (*B*) Shown are results in the presence of 66 μM NQNO at ambient redox potentials of (from top to bottom) +414, +200, +15, −61, −97, −217, and −337 mV.

a potential close to that seen in the untreated state. Because the pH dependence of the high-potential (HP) wave seemed to be substantially different from that obtained on the noninhibited enzyme, Alric *et al.* argued that this HP species probably represented a different state of heme c_i in the presence of NQNO rather than merely a fraction of complex that did not bind the inhibitor.

The presence of two populations of heme c_i titrating in the presence of NQNO at potentials above and below, respectively, the midpoint potential of the close-by heme b_H [−20 mV (3)] provides a powerful experimental tool to detect and investigate possible interactions between the two cofactors.

Comparison of spectra recorded at different redox potentials in the presence of NQNO (Fig. 3*B*) demonstrated that, rather than simply decreasing in amplitude upon progressive reduction, heme c_i's signals in the $g = 6$ region dramatically changed shape in the course of the titration. Below +15 mV, the spectrum transformed to that of a typical rhombic high-spin heme and vanished upon further reduction without distinguishable spectral changes. A spectral conversion is therefore superimposed on the decrease in amplitude.

Fig. 4*A* shows the difference spectra of the HP and the low-potential (LP) compounds observed in this titration above and below the region of ambient potentials where the spectral conversion occurs. The spectrum of the LP component (−217 mV minus −337 mV; LP in Fig. 4*A*) indeed corresponded to a rhombic, noninteracting $S = 5/2$ paramagnetic center with $g_x = 6.3$, $g_y = 5.5$ (rhombicity 5%). The spectrum of the HP compound (+414 mV minus +200 mV; HP in Fig. 4*A*), by contrast, showed two lines symmetrically split about $g = 6.3$ with a splitting constant of 7.5 mT. The g_y signal remained unchanged at $g = 5.5$. Reduction of other redox centers in the enzyme thus obviously had removed a paramagnetic interaction pattern on heme c_i's EPR spectrum. The HP and LP components both show spectra that are significantly different from that seen in the uninhibited enzyme and thus confirm the proposal put forward by Alric *et al.* (3) that the HP electrochemical component corresponds to a

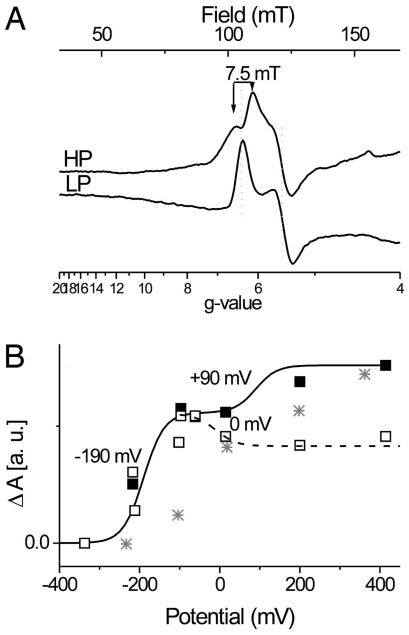

Fig. 4. Evaluation of c_i's redox behavior. (*A*) Redox-induced EPR difference spectra of the high-spin heme signals of the isolated b_6f complex from *C. reinhardtii* in the presence of 66 μM NQNO are shown; HP is +414/+200 mV; LP is −217/−337 mV. EPR settings are as for Fig. 1. (*B*) Signal amplitudes are plotted versus ambient redox potential: ■, g_y signal at 5.5; □, difference of the amplitudes of the g_x signals at 6.5 and 6.1. Two $n = 1$ Nernst curves were fitted to each set of data points. Asterisks indicate signal amplitude of the g_y signal at 5.32 from the titration without inhibitor versus ambient redox potential.

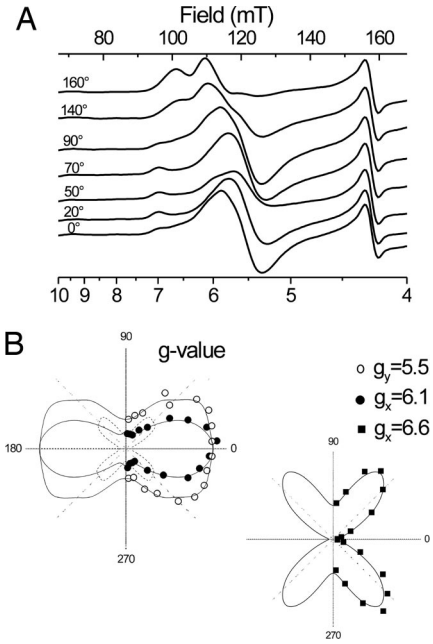

Fig. 5. Orientation of c_i's g tensor in the presence of NQNO. (*A*) EPR spectra were recorded on partially ordered multilayers of chloroplast membranes from spinach in the presence of NQNO. The angle between the magnetic field and the membrane plane is indicated for each spectrum. EPR settings are as for Fig. 1 except for temperature (6 K) and microwave power (63.8 mW). (*B*) Polar plots of signal amplitudes are shown.

second population of heme c_i with NQNO present in the Q_i pocket.

A comparison of the spectral features of the HP and LP species shows that the derivative-shaped g_y line at $g = 5.5$ is not measurably affected during the spectral conversion. We therefore used the amplitude of this line to estimate heme c_i's redox potential dependence (■ in Fig. 4*B*). The data points indicate the presence of two waves separated by a plateau in the region of −100 to 0 mV. In the region of the HP wave the scarcity of data points did not permit the determination of an E_m value. EPR experiments on highly concentrated purified enzyme require vast amounts of sample, precluding a precise titration over the whole redox range (>400 mV) by EPR. We therefore used the value of +90 mV obtained by optical spectroscopy (3) for the HP wave. The simulation of the LP wave required a lower E_m value (−190 mV) than that obtained in the optical study (−130 mV).

The conversion of the split g_x peak of the HP form to the simple g_x peak of the LP form was evaluated by plotting the amplitude difference between the $g = 6.1$ peak of the HP spectrum and the $g = 6.3$ of the LP spectrum versus ambient potential. The resulting curve (□ in Fig. 4*B*) consists of the titration of (*i*) the redox state of the LP species and (*ii*) the spectral conversion corresponding to the decrease in signal amplitude at higher redox potentials. This conversion occurs at an E_m value of ≈0 mV, which is close to the midpoint potential of heme b_H (−20 mV) as determined by Alric *et al.* (3) and is incompatible with any other redox cofactors of the enzyme. These results thus clearly identify heme b_H as the redox center inducing the observed interaction phenomena on heme c_i's EPR spectrum.

Orientation of the *g*-Tensor Axes of Heme c_i in the Presence of NQNO. Fig. 5*A* shows selected EPR spectra of partially ordered membranes from spinach chloroplasts in the presence of NQNO at various orientations with respect to the magnetic field. Fig. 5*B* shows the corresponding polar plots for the peaks at $g_{x1} = 6.6$ and $g_{x2} = 6.1$ and the derivative signal at $g_y = 5.5$. Both g_x signals are similarly oriented, i.e., parallel to the plane of the membrane. g_x and g_y axes of hemes are parallel to the heme plane and perpendicular to each other. Because g_x was found parallel to the membrane, the orientation of the g_y signal directly yields the inclination angle of the heme plane toward the membrane. The angle of 50° determined from this study is in good agreement with heme c_i's inclination, observed in the crystal structure (56°), and thus further confirmed the attribution of these spectral features to heme c_i. The identical orientation of the signals at $g = 6.6$ and 6.1 corroborated our interpretation that they represent a single g_x signal split by magnetic interaction with the closeby heme b_H.

The signal at $g = 6.1$ was superimposed by a composite g_x/g_y signal at $g = 6$ of an axial high-spin center resulting in the apparent difference between the angular dependences of the $g = 6.1$ and $g = 6.6$ signals. Subtracting the curve obtained for the $g = 6.6$ peak from that of the $g = 6.1$ signal revealed a single orientation of the axial $g = 6$ component at 45° (dashed line in Fig. 5*B*). Both in-plane directions, g_x and g_y, are therefore oriented at 45° with respect to the membrane, requiring that the parent heme is perpendicular to the membrane. Possible candidates for this heme species are the high-spin form of either cytochrome b_{559} (7) or cytochrome b_L (8).

Minor signals such as the peak at $g = 7.0$ and shoulders at $g = 5.4$, 5.7, and 6.4 may originate from different substates of heme c_i in the presence of NQNO, from a Q_i site devoid of NQNO or other high-spin species present in the chloroplast membrane. Currently, we cannot distinguish between these possibilities.

Characterization of Heme c_i in the Uninhibited Cytochrome b_6f Complex. EPR spectra in the magnetic field region of g_x/g_y lines from high-spin centers taken at specific ambient potentials are shown in Fig. 3*A*. In contrast to the NQNO-inhibited case where a

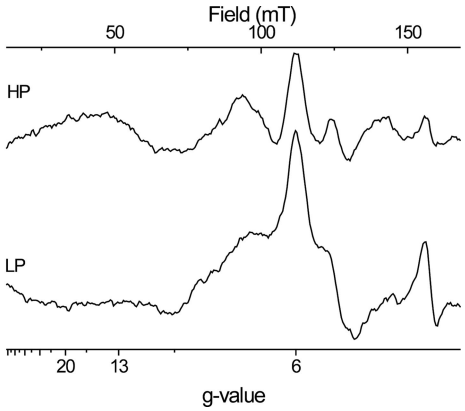

Fig. 6. Difference spectra of HP and LP components. Redox-induced EPR difference spectra of the high-spin heme signals of the isolated b_6f complex from *C. reinhardtii* are shown: HP, +362/+18 mV; LP, +18/−104 mV. EPR settings are as for Fig. 1.

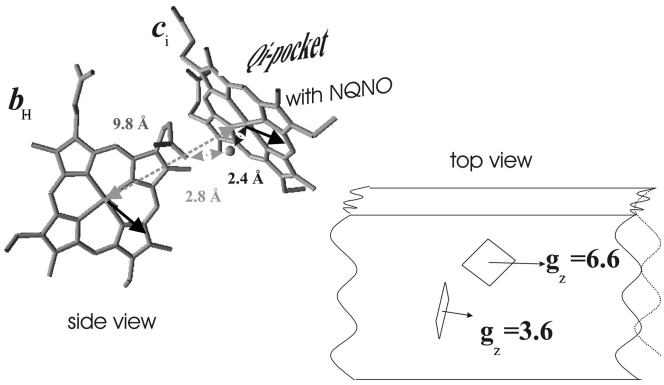

Fig. 7. *g*-tensor orientation with respect to the 3D structure. (*Left*) Structure of the c_i/b_H pair. The oxygen atom bridging heme c_i's central Fe atom to a propionate side-chain oxygen of heme b_H (Protein Data Bank ID code 1Q90) is highlighted. Bold arrows indicate the orientations of b_H's g_z and c_i's g_x directions. (*Right*) Schematic representation of the mutual orientations of the c_i/b_H pair and their maximal *g* values as seen from the n-side of the membrane.

significant fraction of heme c_i was still oxidized at around −100 mV (Figs. 3*B* and 4*A*), virtually no signal intensity remained at comparable potentials in the uninhibited enzyme (Fig. 3*A*). At first sight, this redox behavior seems to be in line with the results of the optical study where only a single HP wave at +100 mV (at pH 7) was observed. However, the amplitudes of the high-spin signals diminished over the entire titration range from +360 mV down to −100 mV, strongly deviating from a single $n = 1$ Nernst curve (Fig. 4*B* see asterisks). For instance, in the spectrum taken at +200 mV, part of the amplitude of the high-spin signals disappeared with respect to the spectrum taken at +362 mV, indicating that a population of heme c_i titrates at much higher E_m values than observed by Alric *et al.* (3). Furthermore, the spectral shape changed during the titration. Redox difference spectra shown in Fig. 6 were calculated from spectra recorded at relatively high (+362 mV minus +18 mV) and moderately low ambient redox potentials (+18 mV minus −104 mV). The broad signals at 50 mT ($g = 13$) and 140 mT ($g = 4.8$) were present mainly in the former difference spectrum. Additionally, both spectra differed in the width of the derivative-shaped line at $g = 5.7$ and the shape of the poorly resolved feature between 80 and 110 mT ($g = 8.5$ and 6.1). Unfortunately, the orientation of c_i signals in uninhibited b_6f complex could not be determined. Preparation of oriented membrane multilayers from these samples resulted repeatedly in loss of the spectral features from heme c_i that were observed in frozen solutions. Instead, a nearly axial, unsplit $g = 6$ signal appeared. A regrettable experimental obstacle at first sight, this behavior may hold information on the environment of heme c_i. Q_i site occupancy by NQNO obviously stabilizes the otherwise more labile environment of heme c_i.

Discussion

Astonishing as heme c_i was to the "functionalists" in the b_6f field, it also provided a major surprise to the metalloenzyme community in general. Its single thioether linkage, the absence of axial ligands arising from the protein, and the presence of a water molecule or hydroxide ion as putative fifth ligand are unique properties for heme proteins. This H_2O/OH^- is in hydrogen-bonding distance to one of the propionate oxygens of heme b_H, and the Fe–Fe distance between c_i and b_H (9.8 Å) is among the shortest observed so far for pairs of hemes. All of these characteristics together with the almost perpendicular arrangement of hemes c_i and b_H make the c_i/b_H pair a unique configuration of redox centers. Accordingly, the magnetic properties of heme c_i, or more appropriately of the c_i/b_H pair, are quite particular.

The Spectral Properties of the NQNO-Inhibited Sample Can Be Rationalized by Magnetic Dipolar Coupling. The results detailed above on the NQNO-treated enzyme showed that at all potentials where heme b_H is oxidized and thus paramagnetic heme c_i's g_x peak is split in two, indicative of coupling to an $S = 1/2$ spin. The fact that this putative coupling disappeared with the reduction of heme b_H would identify the latter as the interaction partner.

Two terms in the Hamiltonian operator of spin pairs are susceptible to inducing spectrally detectable interactions, magnetic dipolar interaction and spin exchange interaction. A rigorous determination of the respective sizes of these interactions at all *g* factors requires, in addition to 3D structural details of the interacting pair, the knowledge of the orientations of the corresponding *g* tensors with respect to the heme systems and to each other, parameters that usually are not accessible for most experimental cases. For the c_i/b_H pair, combining the crystal structure information and the results described above on partially ordered NQNO-inhibited membranes allow the determination of almost all relevant geometric parameters (i.e., direction cosines) of the spin pair. As detailed in *Results*, the data obtained on oriented samples unequivocally positioned the full *g* tensor of heme c_i with respect to the 3D structure. Heme b_H being a typical low-spin heme, its g_z direction must be close to collinear with the heme normal (9) and is thus determined by the 3D structure. The only free variables are the orientations of heme b_H's g_y and g_x axes, which are constrained to lie in the heme b_H plane and to be mutually perpendicular. This fact allows one to calculate the set of possible solutions for the magnetic dipolar interaction by rotating the g_x/g_y diad about b_H's heme normal. Most conveniently, in the case of heme c_i's g_x direction, i.e., the spectral position where an interaction pattern is observed experimentally, the solution is nearly insensitive to the positioning of heme b_H's g_x/g_y diad. The geometric rationalization is illustrated in Fig. 7. As is evident from Fig. 7, heme c_i's g_x and heme b_H's g_z directions are close to collinear, which in turn translates into the magnetic dipolar interaction on heme c_i's g_x value being dominated by heme b_H's g_z value. g_z being heme b_H's maximal *g* value, the magnetic dipolar interaction visible on the g_x peak of heme c_i thus comes close to the maximal interaction possible for this pair of hemes. The absolute maximum value, assuming full collinearity of g_x (c_i) and g_z (b_H), obtained by solving the H_{dd} component of the Hamiltonian operator, is 11 mT. Taking into account a possible deviation of g_z (b_H) from the heme normal (<15°) (10) and the uncertainties inherent in the data obtained on oriented membranes (<10°), the experimentally observed

value of 7.5 mT is perfectly among the solutions that can be obtained for H_{dd}. The interaction pattern visible on heme c_i's EPR spectrum in the g_x region can therefore be explained by magnetic dipolar interaction within the c_i/b_H pair. Heme b_H's spectrum should in turn exhibit additional structure because of the interaction with the spin 5/2 system of heme c_i. A splitting of b_H's g_z peak into several lines is indeed observed in the difference spectum of heme b_H in the NQNO-inhibited enzyme (data not shown).

Multiple Populations of Heme c_i in the Uninhibited State. In the native enzyme, heme c_i titrates almost entirely above heme b_H, precluding straightforward identification of interaction-induced lines. Furthermore and in contrast to the NQNO-inhibited state, too many lines are present to be rationalized solely by interaction with heme b_H. All of these lines indeed arise from heme c_i because they disappear entirely after addition of NQNO (Fig. 2). We can only interpret this multitude of lines by the presence of several distinct subpopulations of heme c_i. The actual existence of such subpopulations is evidenced both by distinguishable spectra in the HP and LP part of heme c_i's redox titration (Fig. 6) and by the weak slope of the redox titration that cannot be fitted by a single $n = 1$ Nernst curve. This observation constitutes a conflict between the optical data by Alric *et al.* (3) who found a single $n = 1$ wave with an E_m of +100 mV, whereas our titration curve extends from +300 to −100 mV. This discrepancy, however, can be rationalized by the different experimental methods. In the optical study, heme c_i is a weak spectral component superimposed on the much larger signals of hemes b_H, b_L, and *f*. In the presence of heterogeneity, the optical approach is likely to reveal only the major, dominant population. In EPR spectra, by contrast, heme c_i's g_x and g_y peaks show up in a spectral region free of contributions of the other hemes (see Fig. 1), at least if the latter are in their undamaged states. Because of the high transition probability of high-spin paramagnetic centers as compared with low-spin systems, heme c_i's spectra are of significant size. Unfortunately, estimation of stoichiometries is much less straightforward in EPR than in optical spectroscopy. Nevertheless, from its large integrated signal intensity, the center giving rise to the broad signal at 50 mT probably represents the major population of heme c_i. This spectral population was found to titrate >0 mV (Fig. 4). It therefore seems well possible that this EPR species corresponds to Alric *et al.*'s (3) +90 mV component, whereas the other centers represent minor populations of heme c_i that escaped attention in the optical study.

Heme c_i's EPR Parameter in the Uninhibited State. In addition to heterogeneity, rhombic distortion and spin–spin interactions (as observed for the NQNO-treated sample) will increase the number of lines deviating from the spectral position at $g = 6$ typical for axial $S = 5/2$ systems. Rhombicity alone cannot shift signals low field beyond $g = 10$ (11). By contrast, lines arising from heme c_i are observed down to 50 mT ($g = 13.5$ in X band). It seems highly unlikely that these low-field lines arise from an $S > 5/2$ spin system because the presence of a sizeable low-spin g_z signal of the potential interaction partner, heme b_H (data not shown), argues against the regrouping of hemes c_i and b_H into a common spin system. Because the results obtained on the NQNO-inhibited sample demonstrate that spin–spin interactions do occur in the c_i/b_H moiety, the signals at apparently very high *g* most probably represent the low-field lines of a splitting imparted by spin–spin interaction on a $g_x < 10$ peak of a rhombic $S = 5/2$ system.

At present, we are unable to propose a reliable attribution of lines to distinct paramagnetic centers in the presence of spin–spin coupling. Too many lines and thus too many possible configurations can be envisaged from the spectra. Several experimental methods in principle lend themselves for sorting out the spectral interpretation of the high-spin species in the uninhibited state, such as S- or Q-band EPR, analysis of oriented samples, and EPR on single crystals. So far, all three approaches have failed to yield conclusive results because of insufficient sample concentrations (for the multifrequency and single-crystal approaches) or lability of the uninhibited complex to drying on Mylar.

This ambiguity of spectral attribution not withstanding, a clear-cut conclusion can be drawn concerning the lower limit of coupling strength. Because the center of coupling-induced pairs of lines cannot exceed $g = 10$, the presence of the peak at 50 mT requires the splitting to be >80 mT. The maximally possible magnetic dipolar coupling constant in this system (assuming $g_x = 10$ for heme c_i and a geometry of *g* tensors as seen in the NQNO-inhibited state) is ≈20 mT. This finding implies that spin exchange interaction with an unusually strong coupling constant *J* should play an important role in the b_H/c_i heme pair.

On the Role of the Bridging H_2O/OH^- Molecule. In the 3D structure, heme c_i was found to be devoid of axial ligands provided by the parent polypeptide chain. An oxygen atom arising from H_2O or OH^-, however, is seen in a position appropriate for an axial ligand (Fig. 7). The high-spin state observed by EPR shows that heme c_i is indeed five-coordinated and thus confirms the role of this oxygen as the fifth ligand on the heme side distal to the Q_i pocket. As discussed above, the EPR spectra recorded on the uninhibited complex clearly indicate heterogeneity in the population of oxidized heme c_i. A rationalization for this heterogeneity that easily comes to mind would consist of OH^- being the fifth ligand in part of the centers and H_2O in others. However, varying the pH between 6 and 9 resulted in only minor spectral modifications (data not shown), and we are therefore reluctant to assume different protonation states of the fifth ligand as the molecular basis for this heterogeneity. The fact that OH^- is a stronger axial ligand than H_2O and that furthermore no model substance has so far been reported that contains H_2O as the fifth axial ligand in a five-coordinated Fe-porphyrin system indicates that in the uninhibited complex the oxygen atom seen in the structure most likely belongs to an OH^- ion. The heterogeneity remains an open issue. It might be caused by different occupancies of the Q_i site.

The addition of NQNO fully abolishes all heterogeneity. Because NQNO is situated in the Q_i pocket, i.e., distal to the oxygen atom of the H_2O/OH^- molecule, a steric influence of NQNO on this latter molecule appears unlikely. To explain the dramatic effect on the EPR spectrum, NQNO must therefore itself ligate to heme c_i. Despite this introduction of a "sixth" ligand, the EPR spectrum remains that of a high-spin state. The binding of NQNO thus either displaces the former fifth ligand or this ligand now binds very weakly to heme c_i. The latter scenario would be in line with a water molecule because, for example, methemo/myoglobins have been shown to accommodate H_2O molecules as sixth ligands while still remaining in the high-spin state (12). Coordination of NQNO to heme c_i suggests a similar mode of binding for plastoquinone. An electron density near c_i's iron was seen in ref. 2 but could not be unambiguously attributed to (possibly coordinated) quinone because of limited resolution.

The strongly decreased bond strength of the oxygen ligand on the heme side opposite to the Q_i pocket upon binding of NQNO is paralleled by the loss of the very strong EPR coupling. In our mind, this fact emphasizes the important role of the bridging OH^-/H_2O molecule in setting up the strongly interacting c_i/b_H pair. It is tempting to speculate that, in addition to mediating spin–spin interactions, this bridging molecule may play a role in interconnecting redox properties of both hemes resulting in the seemingly contradictory redox potentials for heme c_i, ranging from $\ll -50$ mV (4) through −60 mV (13) to +90 mV (3). A tunable midpoint potential for heme c_i would argue for a role in Q_i site turnover,

rather than in redox signaling or cyclic electron transfer. In such a scenario, the b_H/c_i pair may provide both electrons required to fully reduce plastoquinone, explaining the apparent absence of a semiquinone in the Q_i site of b_6f complexes.

Materials and Methods

The cytochrome b_6f complex was purified from *C. reinhardtii* as described by Stroebel *et al.* (2). EPR spectra were recorded on an ESP300e X-band spectrometer (Bruker, Karlsruhe, Germany) fitted with an He-cryostat and temperature control system (Oxford Instruments, Oxon, U.K.). Redox titrations were performed as described by Dutton (14) in the presence of mediators (100 μM Cresyl Blue, anthraquinone, indigocarmine, 2,5-dimethyl-*p*-benzoquinone, and 50 μM ferricyanide). Reductive titrations were carried out with sodium dithionite, and oxidative titrations were carried out using ferricyanide. NQNO was synthesized in the laboratory according to the procedure described in ref. 5. It was used at a concentration of 66 μM during the redox titration; the protein concentration was 30 μM. All experiments were carried out at pH 7.

Chloroplasts were prepared from local market spinach. Two kilograms of spinach leaves were stripped from their nervures and homogenized in a precooled blender in 1 liter of 0.2 M sucrose, 10 mM NaCl, and 50 mM Tris at pH 8. The mixture was filtered through three layers of nylon cloth, centrifuged at 4,300 $\times$ *g* for 10 min, and resuspended in the same buffer. For the preparation of chloroplast membranes, chloroplasts were broken by an osmotic shock in a large excess of 50 mM Mops buffer at pH 7 and 2 mM EDTA and centrifuged at 290,000 $\times$ *g* for 1 h. The upper dark-green layer of the pellet was used for the experiments. Partially ordered chloroplast membrane multilayers were prepared by an additional washing step of those membranes in doubly distilled water at pH 7, before painting them on Mylar sheets (15).

We thank R. Kappl (University of Homburg, Homburg, Germany) for stimulating discussions and suggestions and the group of B. Guigliarelli (Laboratoire de Bioénergétique et Ingénierie des Protéines, Centre National de la Recherche Scientifique) for extensive access to the EPR facilities.

1. Kurisu G, Zhang H, Smith JL, Cramer WA (2002) *Science* 302:1009–1014.
2. Stroebel D, Choquet Y, Popot J-L, Picot D (2003) *Nature* 426:413–418.
3. Alric J, Pierre Y, Picot D, Lavergne J, Rappaport F (2005) *Proc Natl Acad Sci USA* 102:15860–15865.
4. Zhang H, Primak A, Cape J, Bowman MK, Kramer DM, Cramer WA (2004) *Biochemistry* 43:16329–16336.
5. Cornforth JW, James AT (1956) *Biochem J* 63:124–130.
6. Musser SM, Stowell HB, Lee HK, Rumbley JN, Chan SI (1997) *Biochemistry* 36:894–902.
7. Rutherford AW (1985) *Biochim Biophys Acta* 807:189–201.
8. Nitschke W, Hauska G (1987) *Biochim Biophys Acta* 892:314–319.
9. Mailer C, Taylor CP (1972) *Can J Biochem* 50:1048–1055.
10. Hori H, Fujii M, Shiro Y, Iizuka T, Adachi S, Morishima I (1989) *J Biol Chem* 264:5715–5719.
11. Hagen WR (1992) in *Advances in Inorganic Chemistry*, eds Cammack R, Sykes AG (Academic, San Diego), pp 165–222.
12. Bennett JE, Gibson JF, Ingram DJE (1957) *Proc R Soc London Ser A* 240:67–82.
13. Lavergne J (1983) *Biochim Biophys Acta* 725:25–33.
14. Dutton PL (1971) *Biochim Biophys Acta* 226:63–80.
15. Rutherford AW, Sétif P (1990) *Biochim Biophys Acta* 1100:128–132.